Original Article

Honeycomb lung is a major risk factor for preoperative radiological tumor size underestimation in patients with primary lung cancer

Hisato Ishizawa[1], Yasushi Matsuda[1], Yoshiharu Ohno[2], Eiko Sakurai[3], Atsuhiko Ota[4], Hidekazu Hattori[2], Tetsuya Tsukamoto[3], Masaaki Matsunaga[4], Hiroshi Kawai[1], Yamato Suzuki[1], Hiromitsu Nagano[1,5], Takahiro Negi[5], Daisuke Tochii[5], Sachiko Tochii[5], Takashi Suda[5], Yasushi Hoshikawa[1]^

[1]Department of Thoracic Surgery, Fujita Health University, Toyoake, Japan; [2]Department of Radiology, Fujita Health University, Toyoake, Japan; [3]Department of Diagnostic Pathology, Fujita Health University, Toyoake, Japan; [4]Department of Public Health, Fujita Health University, Toyoake, Japan; [5]Department of Thoracic Surgery, Fujita Health University Okazaki Medical Center, Okazaki, Japan

Contributions: (I) Conception and design: H Ishizawa, Y Ohno, Y Hoshikawa; (II)Administrative support: None; (III) Provision of study materials or patients: None; (IV) Collection and assembly of data: H Ishizawa, Y Ohno, E Sakurai, H Hattori, T Tsukamoto; (V) Data analysis and interpretation: H Ishizawa, Y Matsuda, Y Ohno, A Ota, M Matsunaga; (VI) Manuscript writing: All authors; (VII) Final approval of manuscript: All authors.

Correspondence to: Yasushi Hoshikawa, MD, PhD. Department of Thoracic Surgery, Fujita Health University, 1-98 Dengakugakubo, Kutsukake-cho, Toyoake 470-1192, Japan. Email: yasushih@fujita-hu.ac.jp.

Background: Lung cancer frequently occurs in lungs with background idiopathic interstitial pneumonias (IIPs). Limited resection is often selected to treat lung cancer in patients with IIPs in whom respiratory function is already compromised. However, accurate surgical margins are essential for curative resection; underestimating these margins is a risk for residual lung cancer after surgery. We aimed to investigate the findings of lung fields adjacent to cancer segments affect the estimation of tumor size on computed tomography compared with the pathological specimen.

Methods: This analytical observational study retrospectively investigated 896 patients with lung cancer operated on at Fujita Health University from January 2015 to June 2020. The definition of underestimation was a ≥10 mm difference between the radiological and pathological maximum sizes of the tumor.

Results: The lung tumors were in 15 honeycomb, 30 reticulated, 207 emphysematous, and 628 normal lungs. The ratio of underestimation in honeycomb lungs was 33.3% compared to 7.4% without honeycombing (P=0.004). Multivariate analysis showed that honeycombing was a significant risk factor for tumor size underestimation. A Bland-Altman plot represented wide 95% limits of agreement, –40.8 to 70.2 mm, between the pathological and radiological maximum tumor sizes in honeycomb lungs.

Conclusions: Honeycomb lung adjacent to the tumor is a major risk factor for preoperative radiological tumor size underestimation in patients with lung cancer.

Keywords: Idiopathic interstitial pneumonia; underestimation; tumor size; honeycomb lung; honeycombing

Submitted Aug 13, 2022. Accepted for publication Jan 06, 2023. Published online Feb 21, 2023.
doi: 10.21037/jtd-22-1115
View this article at: https://dx.doi.org/10.21037/jtd-22-1115

^ ORCID: 0000-0003-3235-8253.

Introduction

The incidence of lung cancer in the patients with idiopathic interstitial pneumonias (IIPs) is reportedly as high as 15% (1). IIPs, especially idiopathic pulmonary fibrosis (IPF), are characterized by honeycombing resulting from alveolar fibrosis (2). Sakai *et al*. showed that lung cancer in the honeycomb lung progressed along with reticulated fibrotic lung tissue and collapsed alveoli, so the border between the tumor and fibrotic lung tissue was unclear radiologically (3). Therefore, it is difficult to estimate tumor extension adjacent to fibrotic lung tissue through computed tomography (CT) images (4). Fukui *et al*. showed the risk of preoperative underestimation of tumor size in patients with IIPs was high (5).

Patients with IIPs may sometimes have limited respiratory function, often resulting in surgeons selecting a limited resection such as sub-lobar resection to treat lung cancer complicated by IIPs (6,7). In addition, postoperative acute exacerbation (AE) of IIPs is a life-threatening complication (6). Sato *et al*. advocated for a risk-scoring system to predict AEs of IIPs after pulmonary resection for lung cancer, in which surgical procedures, other than wedge resection, were one of the major predictors for AE (8). They suggested that a limited resection was recommended for high-risk patients to reduce the risk of AE (8). However, the possible preoperative underestimation of tumor size could result in incomplete tumor resection (5).

The lung fields of the patients with IIPs show not only honeycombing but also reticulation and emphysema; they may even be normal (9). It is unclear which findings of the lung field adjacent to cancer segments may affect tumor size assessment. Therefore, this study aimed to investigate whether findings of lung fields adjacent to cancer segments, including honeycombing, could cause underestimation of tumor size on CT images when compared to the pathological specimen. We present the following article in accordance with the STROBE reporting checklist (available at https://jtd.amegroups.com/article/view/10.21037/jtd-22-1115/rc).

Highlight box

Key findings

- Honeycomb lung adjacent to lung cancer frequently causes radiological tumor size underestimation.

What is known and what is new?

- Risk of preoperative underestimation of tumor size in patients with lung cancer complicated with idiopathic interstitial pneumonias was reported to be high.
- This manuscript shows honeycomb lung adjacent to the tumor is a major risk factor for preoperative tumor size underestimation.

What is the implication, and what should change now?

- A suitable resection method should be selected to ensure a curative operation for lung cancer adjacent to honeycomb lung. Meanwhile, more accurate diagnostic tools to determine the extension of lung cancer into the adjacent honeycomb lung should be developed.

Methods

Study design

This retrospective observational study was conducted in accordance with the ethical standards of the Declaration of Helsinki (as revised in 2013). This study was approved by the Institutional Review Board of Fujita Health University (CI21-392). The patients viewed an online version of the consent document and were enrolled in the study using the opt-out method.

Patient population

We investigated 896 patients with primary lung cancer who underwent lung resection between January 2015 and June 2020 in the Department of Thoracic Surgery, Fujita Health University Hospital, Japan. This study size was reasonable considering frequency of surgical intervention for patients who have honeycomb lung in our institution. Patients who received preoperative chemotherapy and/or radiotherapy were excluded. Patients who had radiological findings other than normal, emphysematous, reticulated, or honeycombing areas adjacent to the tumor were excluded.

Definition of preoperative underestimate of tumor size

We defined it as the underestimation of ≥10 mm in pathological maximum tumor dimension compared with radiological one.

Preoperative radiological assessment and background lung assessment

Two board certified chest radiologists with more than 20 years experiences reviewed all CT images and classified the background lung according to eight patterns; normal lung, bronchiectasis, consolidation, emphysema, ground-glass

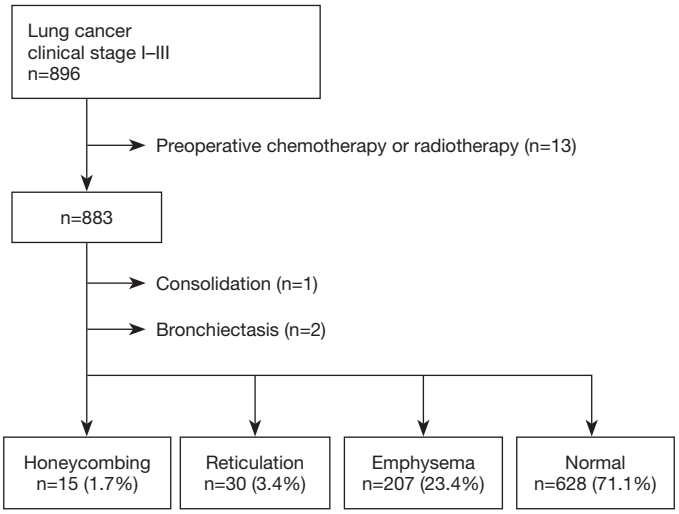

Figure 1 Flow diagram for subjects' selection.

opacity, honeycombing, nodular lesion, reticulation based on the glossary of Flesichner Society (10). Preoperative tumor size was determined based on radiological reports from at least two radiologists. The largest diameters were measured on 0.5–7.0-mm CT images at axial plane with or without 0.5–5.0-mm multiplanar reconstruction (MPR) images at coronal or sagittal planes with lung window setting (width, 1,600 HU; level, −600 HU). Tumors close to the chest wall and mediastinum were also measured at a mediastinal window setting (width, 300 HU; level, 30 HU). These measurements were also checked in our thoracic surgeon conferences. We restaged the cases after 2018 according to the 7th Edition of TNM in Lung Cancer of International Association for Study of Lung Cancer (IASLC).

Pathological assessment

Ten percent buffered formalin was injected into wedge resection specimens using needle, or into segmentectomy, lobectomy, and pneumonectomy specimens from the bronchial stump soon after excision. After inflation of the lung, the specimen was soaked in 10% buffered formalin. All specimens were evaluated by three pathologists. Pathological tumor size was evaluated with hematoxylin and eosin staining (H&E) microscopically. We reviewed all pathological reports and restaged the cases after 2018 according to the 7th Edition of TNM in IASLC.

Statistical analysis

We divided the patients by each radiological finding and the presence or absence of underestimated tumor size. The difference between these groups was compared using chi-square tests, student *t*-tests, Bonferroni correction, Spearman's rank correlation coefficient, and logistic regression analysis. All P values were two-sided, and P values of 0.05 or less were considered statically significant. A Bland-Altman plot (11) was constructed with Excel for Mac version 16.62 (Microsoft Corporation, Redmond, WA, USA). All other statistical analyses were performed with EZR (12) (Saitama Medical Center, Jichi Medical University, Saitama, Japan), which is a graphical user interface for R (version 4.0.0, The R Foundation for Statistical Computing, Vienna, Austria). More precisely, it is a modified version of R commander (version 2.6-2) designed to add statistical functions frequently used in biostatistics.

Results

Overall, 883 patients were classified into four groups according to radiological findings of the lung field adjacent to lung cancer on preoperative chest CT images (honeycombing, n=15, 1.7%; reticulation, n=30, 3.4%; emphysema, n=207, 23.4%; and normal, n=628, 71.1%) (*Figure 1*). Patients with consolidation (n=1) or bronchiectasis (n=2) in the lung field adjacent to lung cancer

were excluded from the subjects. The clinicopathological characteristics of the patients in the four groups are shown in *Table 1*.

Radiological findings adjacent to lung cancer and tumor size underestimation

Preoperative radiological tumor size underestimation of 10 mm or more occurred in 5 patients (33.3%) in the honeycombing group, whereas in 2 (6.7%), 15 (7.2%), and 47 patients (7.5%) in the reticulation, emphysema, and normal lung groups respectively (P=0.003) (*Table 2*). Comparison between the honeycombing group and the group without honeycombing (including the reticulation, emphysema, and normal lung groups) revealed that tumor size underestimation was significantly more frequent in the patients with honeycomb lung adjacent to the tumor (5 out of 15, 33.3%) than in those without honeycombing (64 out of 865, 7.4%) (P=0.004) (*Table 3*).

Risk factors for tumor size underestimation

The results of univariate analysis for the characteristics of the patients with or without tumor size underestimation are shown in *Table 4*. Age, sex, smoking history, tumor location, imaging plane (only axial or axial, coronal or sagittal plane on MPR images), most fine slice width of CT images, surgical procedure (wedge resection or anatomical

Table 1 Clinicopathological characteristics of the patients

Variables	Honeycombing (n=15)	Reticulation (n=30)	Emphysema (n=207)	Normal (n=628)
Age (years)	74.8±5.4	72.3±4.7	70.0±8.0	68.6±9.9
Sex				
Female	3 (20.0%)	8 (26.7%)	22 (10.6%)	309 (49.2%)
Male	12 (80.0%)	22 (73.3%)	185 (89.4%)	319 (50.8%)
Smoking history, pack-year				
<30	2 (13.3%)	14 (46.7%)	26 (12.6%)	418 (67.3%)
≥30	13 (86.7%)	16 (53.3%)	180 (87.4%)	203 (32.7%)
Tumor location				
Upper or middle lobe	6 (40.0%)	6 (20.0%)	153 (73.9%)	398 (63.4%)
Lower lobe	9 (60.0%)	24 (80.0%)	54 (26.1%)	230 (36.6%)
Imaging plane				
Axial plane	5 (33.3%)	4 (13.3%)	31 (15.0%)	84 (13.4%)
MPR[a]	10 (66.7%)	26 (86.7%)	176 (85.0%)	544 (86.6%)
Most fine slice width of CT images (mm)	1.1±1.1	1.9±1.7	1.2±1.1	1.2±1.1
Surgical procedure				
Wedge resection	8 (53.3%)	5 (16.7%)	22 (10.6%)	62(9.9%)
Segmentectomy	1 (6.7%)	0	5 (2.4%)	14 (2.2%)
Lobectomy	6 (40.0%)	24 (80.0)	174 (84.1%)	545 (86.8%)
Pneumonectomy	0	1 (3.3%)	6 (2.9%)	7 (1.1%)
Interval between CT and surgery (days)	40.5±35.7	32.0±19.1	36.2±28.5	37.6±31.7
Radiological maximum tumor size (mm)	20.5±6.1	31.1±18.7	29.7±16.1	24.1±14.1
Pathological maximum tumor size (mm)	35.3±28.0	29.4±14.9	28.6±16.7	22.3±13.8

Table 1 (*continued*)

Table 1 (*continued*)

Variables	Honeycombing (n=15)	Reticulation (n=30)	Emphysema (n=207)	Normal (n=628)
Histological type				
Adenocarcinoma	9 (60.0%)	15 (60.0%)	120 (62.2%)	545 (89.3%)
Squamous cell carcinoma	6 (40.0%)	10 (40.0%)	73 (37.8%)	65 (10.7%)
Lymphovascular invasion				
Positive	7 (46.7%)	15 (50.0%)	73 (35.3%)	137 (21.8%)
Vascular invasion				
Positive	7 (46.7%)	16 (53.3%)	89 (43.0%)	176 (28.0%)
Pleural invasion				
Positive	6 (40.0%)	9 (30.0%)	51 (24.6%)	78 (12.4%)
Histological grade				
1	2 (13.3%)	2 (6.7%)	21 (10.1%)	175 (27.9%)
2	8 (53.3%)	22 (73.3%)	132 (63.8%)	395 (62.9%)
3	4 (26.7%)	5 (16.7%)	42 (20.3%)	49 (7.8%)
4	1 (6.7%)	1 (3.3%)	12 (5.8%)	9 (1.4%)
%VC	101.6±17.6	107.6±21.3	116.2±76.0	112.2±18.4
FEV_1/FVC (%)	77.6±8.4	72.7±14.0	66.3±12.7	74.2±12.6
$\%DL_{CO}$	77.3±20.0	87.1±27.7	87.2±23.8	107.0±24.4
Underestimation of tumor size[b] (mm)	14.7±28.3	−1.7±9.3	−1.1±10.0	−1.7±9.7

Values are shown as number of patients (percentage) or mean ± SD. [a], axial, coronal or sagittal plane on multiplanar reconstruction; [b], pathological maximum tumor size minus radiological maximum tumor size on preoperative CT images. SD, standard deviation; CT, computed tomography; %VC, %vital capacity; FEV_1, forced expiratory volume in 1 second; FVC, forced expiratory volume; $\%DL_{CO}$, %diffusing capacity for carbon monoxide.

Table 2 Preoperative tumor size underestimation in the four groups (honeycombing, reticulation, emphysema, and normal) according to radiological findings of the lung field adjacent to the tumor

Variables	Honeycombing (n=15)	Reticulation (n=30)	Emphysema (n=207)	Normal (n=628)	P value
Underestimated[a]	5 (33.3%)	2 (6.7%)	15 (7.2%)	47 (7.5%)	0.003
Not underestimated	10 (66.7%)	28 (93.3%)	192 (92.8%)	581 (92.5%)	

[a], defined as 10 mm or more in pathological maximum tumor size compared to radiological maximum tumor size on preoperative CT images. CT, computed tomography.

Table 3 Preoperative tumor size underestimation in the two groups (with or without honeycombing) according to radiological findings of the lung field adjacent to the tumor

Variables	Honeycombing (n=15)	Without honeycombing (n=865)	P value
Underestimated[a]	5 (33.3%)	64 (7.4%)	0.004
Not underestimated	10 (66.7%)	801 (92.6%)	

[a], defined as 10 mm or more in pathological maximum tumor size compared to radiological maximum tumor size on preoperative CT images. CT, computed tomography.

Table 4 Characteristics of the patients with or without tumor size underestimation

Variables	Underestimation[a] (n=69)	Without underestimation (n=811)	P value
Age	70 [49, 86]	71 [27, 91]	0.681
Sex			0.521
Female	24 (34.8%)	318 (39.2%)	
Male	45 (65.2%)	493 (60.8%)	
Smoking history, pack-year			0.131
<30	30 (43.5%)	430 (53.5%)	
≥30	39 (56.5%)	373 (46.5%)	
Tumor location			0.434
Upper or middle lobe	41 (59.4%)	522 (64.4%)	
Lower lobe	28 (40.6%)	289 (35.6%)	
Radiological findings[b]			0.004
Honeycombing	5 (7.2%)	10 (1.2%)	
Without honeycombing	64 (92.8%)	801 (98.8%)	
Imaging plane			0.469
Axial plane	117 (14.4%)	7 (10.1%)	
MPR[c]	694 (85.6%)	62 (89.9%)	
Most fine slice width of CT images (mm)	1.14 [0.50, 5.00]	1.22 [0.30, 7.00]	0.554
Surgical procedure			0.421
Wedge resection	5 (7.2%)	91 (11.2%)	
Anatomical resection[d]	64 (92.8%)	720 (88.8%)	
Interval between CT and surgery (days)	36 [1, 167]	27 [0, 37]	0.226
Radiological maximum tumor size (mm)	25.0 [11.0, 84.0]	21.0 [5.0, 111.0]	0.013
Pathological maximum tumor size (mm)	41.0 [25.0, 120.0]	20.0 [1.0, 80.0]	<0.001
Histological type of lung cancer			0.621
Adenocarcinoma	53 (79.1%)	636 (82.0%)	
Squamous cell carcinoma	14 (20.9%)	140 (18.0%)	
Lymphovascular invasion			
Positive	20 (29.0%)	212 (26.1%)	0.669
Vascular invasion			
Positive	25 (36.2%)	263 (32.4%)	0.507
Pleural invasion			
Positive	17 (24.6%)	127 (15.7%)	0.062
Histological grade			0.141
1	9 (13.0%)	191 (23.6%)	
2	49 (71.0%)	508 (62.6%)	

Table 4 (*continued*)

Table 4 (*continued*)

Variables	Underestimation[a] (n=69)	Without underestimation (n=811)	P value
3	8 (11.6%)	92 (11.3%)	
4	3 (4.3%)	20 (2.5%)	
%VC	110.4 [76.6, 158.1]	111.4 [55.3, 175.0]	0.141
FEV_1/FVC (%)	72.9 [40.3, 129.3]	72.4 [29.7, 134.7]	0.419
$\%DL_{CO}$	101.1 [53.5, 198.3]	100.6 [39.1, 199.10]	0.953
Underestimation of tumor size[e] (mm)	14.0 [10.0, 99.0]	−2.0 [−83.0, 9.0]	<0.001

Values are shown as number of patients (percentage) or median value [minimum value, maximum value]. [a], defined as 10 mm or more in pathological maximum tumor size compared to radiological maximum tumor size on preoperative CT images; [b], radiological findings of the lung field adjacent to the tumor on preoperative CT images; [c], axial, coronal or sagittal plane on multiplanar reconstruction; [d], segmentectomy, lobectomy, or pneumonectomy; [e], pathological maximum tumor size minus radiological maximum tumor size on preoperative CT images. %VC, %vital capacity; FEV_1, forced expiratory volume in 1 second; FVC, forced expiratory volume; $\%DL_{CO}$, %diffusing capacity for carbon monoxide. CT, computed tomography.

Table 5 Multivariate analysis of predictors for tumor size underestimation using the logistic regression model

Variables	Odds ratio	95% CI	P value
Honeycombing adjacent to the tumor	8.58	2.49–29.60	0.000659
Surgical procedure (wedge resection)	0.47	0.16–1.35	0.158
Radiological maximum tumor size	1.07	0.91–1.26	0.419
Tumor location (lower lobe)	1.19	0.71–1.99	0.505
Pathological pleural invasion, positive	1.54	0.83–2.86	0.168
Most fine slice width of CT images	0.99	0.72–1.36	0.930
Imaging plane (MPR)	1.46	0.52–4.15	0.475

CI, confidence interval; CT, computed tomography; MPR, multiplanar reconstruction.

resection), interval between CT and surgery, histological type of the tumor (adenocarcinoma or squamous cell carcinoma), pathological lymph-vascular invasion, vascular invasion, histological grade, and preoperative pulmonary function [%vital capacity (%VC), forced expiratory volume in 1 second (FEV_1)/forced expiratory volume (FVC), and %diffusing capacity for carbon monoxide ($\%DL_{CO}$)] were not significantly different between the patients with and without tumor size underestimation. Honeycombing adjacent to the tumor on preoperative CT images was substantially more frequent in the patients with tumor size underestimation than in those without underestimation (P=0.004). The patients with tumor size underestimation had significantly larger radiological (P=0.0013) and pathological (P<0.001) tumor sizes than did those without tumor size underestimation. Pathological pleural invasion of the tumor tended to be observed more frequently in patients with tumor size underestimation than in those without underestimation.

Multivariate analysis using the logistic regression model revealed that honeycombing adjacent to the tumor was a statistically significant predictor for tumor size underestimation (odds ratio, 8.58; 95% CI: 2.49–29.60; P=0.000659) (*Table 5*).

Pathological causes of tumor size underestimation in the honeycombing group

Two representative cases with honeycombing in the lung field adjacent to the tumor, in whom underestimation of tumor size occurred, are shown in *Figure 2*. Histopathological analysis of the first case revealed that

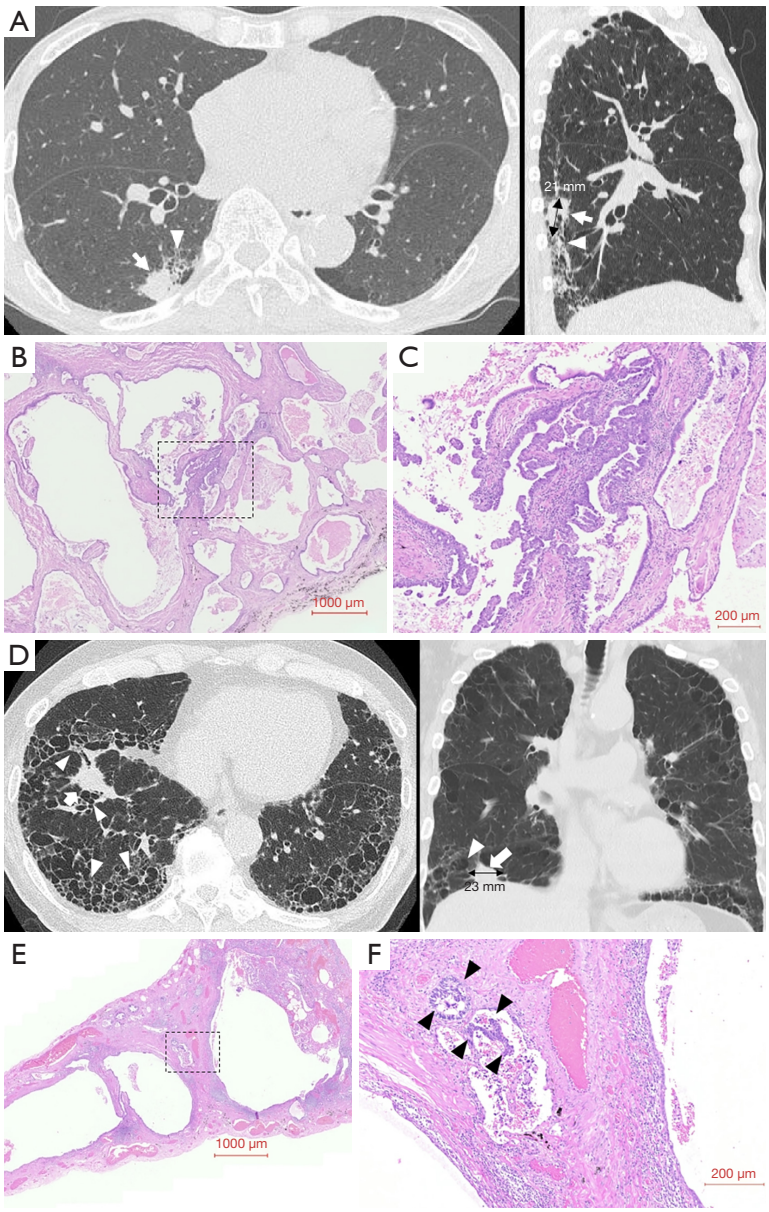

Figure 2 Two representative cases with honeycomb lung adjacent to lung cancer, in whom underestimation of tumor size occurred. (A) Axial (left) and sagittal (right) CT images of Case 1, a 78-year-old man with invasive adenocarcinoma complicated by idiopathic interstitial pneumonia, represent a nodule with spiculation and a maximum diameter of 21 mm in the right lower lobe (arrow). The nodule is adjacent to the honeycomb lung (arrowhead). (B) A low-powered histopathological image of the edge of the nodule in Case 1 shows papillary adenocarcinoma infiltrates on the surface of dilated airway in the honeycomb lung (H&E). (C) An enlarged view of the rectangular area drawn with dashed lines in (B) shows papillary growth of adenocarcinoma cells on the surface of the honeycomb lung (H&E). The pathological maximum size of this adenocarcinoma was 120 mm. (D) Axial (left) and coronal (right) CT images in Case 2, a 69-year-old man with invasive adenocarcinoma complicated by idiopathic interstitial pneumonia, represent a nodule with spiculation and a maximum diameter of 23 mm in the right lower lobe (arrow). The nodule is adjacent to the honeycomb lung (arrowhead). (E) A low-powered histopathological image of the edge of the nodule in Case 2 shows adenocarcinoma extended to fibrotic lung tissue adjacent to honeycomb lung (H&E). (F) An enlarged view of the rectangular area drawn with dashed lines in (E) shows extension of adenocarcinoma cells in the fibrotic tissue between the enlarged airspaces (H&E). The pathological maximum size of this adenocarcinoma was 60 mm. CT, computed tomography; H&E, hematoxylin and eosin staining.

Table 6 Characteristics of patients with tumor size underestimation in the group of honeycombing adjacent to the tumor

Age (years)	Sex	Surgical procedure	Radiological size (mm)[a]	Pathological size (mm)[b]	Histological type of lung cancer	Pathological cause for tumor size underestimation
78	Male	RLL[d]	21	120	Adenocarcinoma	Infiltration to honeycomb lung
69	Male	Wedge[c]	11	65	Adenocarcinoma	Infiltration to honeycomb lung
69	Male	RLL[d]	23	60	Adenocarcinoma	Infiltration to fibrotic lung tissue adjacent to honeycomb lung
81	Female	LLL[e]	19	30	Adenocarcinoma	Infiltration to fibrotic lung tissue adjacent to honeycomb lung
79	Male	RUL[f]	13	26	Adenocarcinoma	Invasion to subpleural cyst

[a], radiological maximum tumor size on preoperative CT images; [b], pathological maximum tumor size; [c], wedge resection; [d], right lower lobectomy; [e], left lower lobectomy; [f], right upper lobectomy. CT, computed tomography.

adenocarcinoma infiltrated along the surface of the dilated airway in the honeycomb lung (*Figure 2B*,*2C*). The radiological maximum tumor size assessed by sagittal plane on the preoperative MPR images was 21 mm (*Figure 2A*), whereas pathological examination showed the actual tumor size was 120 mm. In histology of the second case, adenocarcinoma extended to fibrotic lung tissue adjacent to honeycomb lung (*Figure 2E*,*2F*). The radiological maximum tumor size assessed by coronal plane on the preoperative MPR images was 23 mm (*Figure 2D*), whereas the actual pathological tumor size was 60 mm. The pathological causes for tumor size underestimation in the five cases with honeycombing adjacent to the tumor were tumor infiltration to honeycomb lung in 2 patients, including in *Figure 2A-2C*, tumor extension to fibrotic lung tissue adjacent to honeycomb lung in 2 cases, including in *Figure 2D-2F*, and tumor invasion into a subpleural cyst in 1 case (*Table 6*).

Spearman's correlation analysis and Bland-Altman analysis of pathological and radiological maximum tumor sizes

Next, we created a scatter diagram for the radiological maximum tumor size on the preoperative CT images and the pathological tumor size in the patient groups with (*Figure 3A*) and without (*Figure 3B*) honeycombing adjacent to the tumor. The correlation between the radiological and pathological maximum tumor sizes in the patient group without honeycombing was satisfactory (Spearman's correlation rho =0.831, P<0.0001), but not that with honeycombing (Spearman's correlation rho =0.294, P=0.287).

The mean difference and 95% limits of agreement between the pathological and radiological maximum tumor sizes in two groups of patients with (*Figure 3C*) and without (*Figure 3D*) honeycombing were determined using Bland-Altman analysis. The mean difference between the pathological and radiological maximum tumor sizes in the group with honeycombing (14.7±7.3 mm) was significantly more when compared with that in the group without honeycombing (–1.6±0.3 mm) (P=0.0013). The 95% limits of agreement between the pathological and radiological maximum tumor sizes were 14.7±55.5 (–40.8 to 70.2) mm in the group with honeycombing, whereas –1.6±19.0 (–20.6 to 17.4) mm in the group without honeycombing.

Discussion

The principal findings of this study are as follows: (I) preoperative radiological tumor size underestimation of 10 mm or more on CT images occurred significantly more frequently in the patients with honeycomb lung adjacent to the tumor than in those without honeycombing (i.e., with reticulation, emphysema, or normal lung); (II) multivariate analysis revealed that honeycombing adjacent to the tumor was a statistically significant predictor for preoperative radiological tumor size underestimation; (III) the pathological causes for tumor size underestimation was mainly due to tumor infiltration to honeycomb lung or fibrotic lung tissue adjacent to honeycomb lung, and (IV) Bland-Altman analysis determined the 95% limits of agreement between the pathological and radiological maximum tumor sizes were 14.7±55.5 (–40.8 to 70.2) mm in the patients with honeycombing adjacent to the tumor.

Patients with IPF have a greater risk for lung cancer development (13,14), with relative risks of 7.31–14.1 than the general population, even after accounting for common

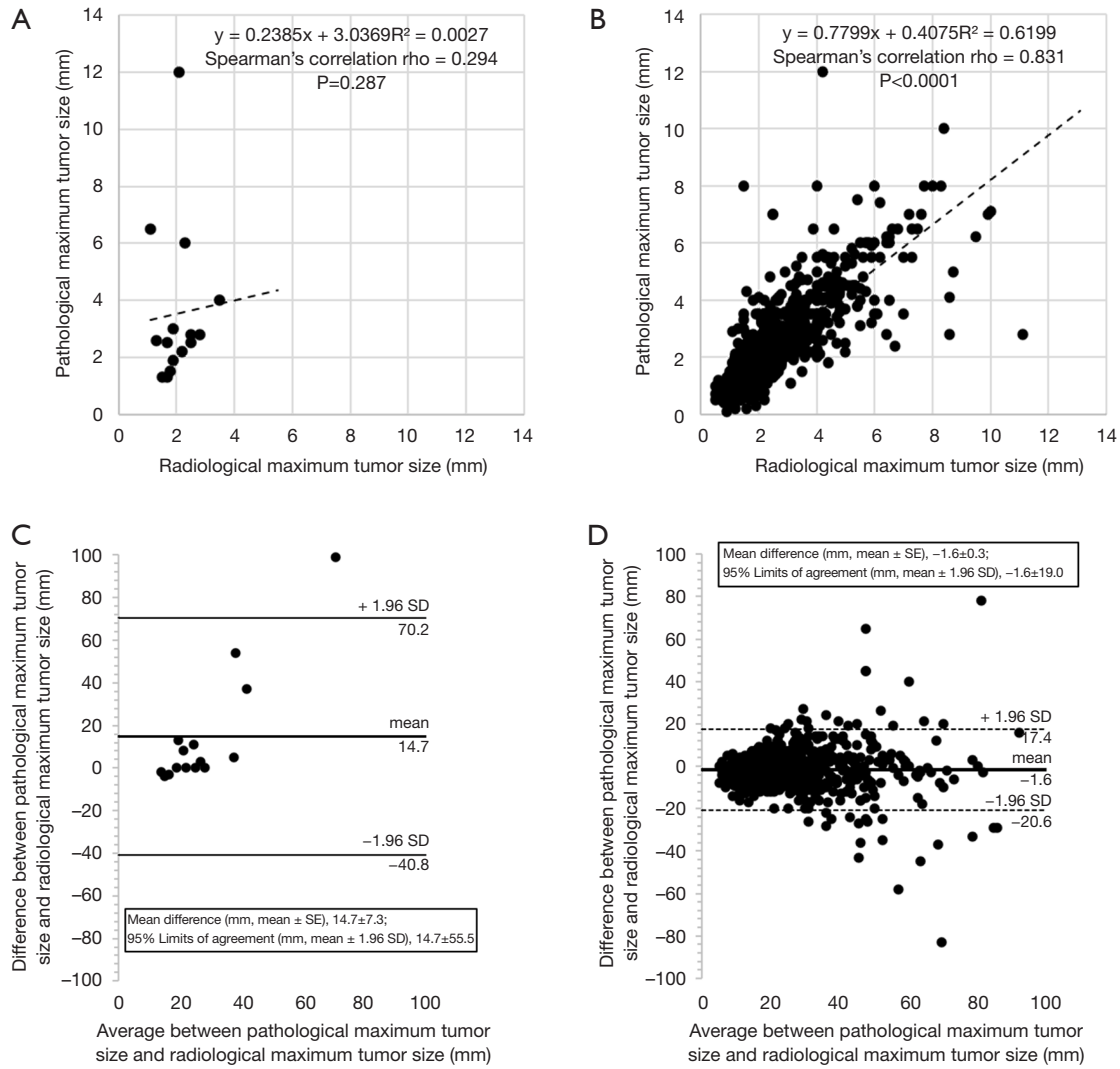

Figure 3 Relationship between radiological maximum tumor size on preoperative CT images (horizontal axis) and pathological maximum tumor size (vertical axis) in patients with honeycombing adjacent to the tumor (A, n=15) and in those without honeycombing (reticulation, emphysema, or normal) (B, n=865). The dashed line represents the regression line (A,B). Determination coefficients (R^2), Spearman's correlation rho, and P values are shown in (A,B). Graphs of Bland-Altman analysis of pathological maximum tumor size and radiological maximum tumor size on preoperative CT images in patients with honeycombing adjacent to the tumor (C, n=15) and in those without honeycombing (reticulation, emphysema, or normal) (D, n=865). The solid horizontal line represents the mean difference (C,D). The top and bottom dashed lines indicate the upper and lower 95% limits of agreement, respectively, and the dots donate data points (C,D). The values of mean difference (mm, mean ± SE) and 95% limits of agreement (mm, mean ± 1.96 SD) are indicated in (C,D). CT, computed tomography; SE, standard error; SD, standard deviation.

risk factors, such as older age and smoking history (1). Limited resection is sometimes selected for the patients with lung cancer complicated with IIPs due to the poor pulmonary function or high risk of AE of IIPs post-surgery (8). In sub-lobar surgery, such as partial resection or segmental resection, we need to focus on accurate assessment of tumor extension and ensuring adequate surgical margins without residual cancer are essential.

Usual interstitial pneumonia is the hallmark radiologic and histopathological pattern of IPF (9). The diagnostic

criterion of usual interstitial pneumonia is a low magnification appearance of patchy dense fibrosis that: (I) causes remodeling of lung architecture; (II) often results in honeycomb change; and (III) alternates with areas of less-affected parenchyma (9). Honeycombing refers to clustered cystic airspaces of typically consistent diameter with thick, well-defined walls, and is usually accompanied by a reticular pattern (10). It has been shown that lung cancer in honeycombed lungs progressed along with reticulated fibrotic lung tissue and collapsed alveoli, until the border between the tumor and fibrotic lung tissue was unclear radiologically (3). Moreover, many patients with IPF also have other comorbid conditions, including emphysema (15), which can cause tumor size underestimation on radiological measurements when compared with pathological ones (16). Therefore, in this study, two radiologists classified the lung background on CT images into four patterns; normal, emphysematous, reticulated, or honeycombing. Subsequently, the ratio of preoperative radiological tumor size underestimation in each group was investigated. The normal, emphysema, and reticulation groups had almost the same low incidence of the tumor size underestimation (7.5%, 7.2%, and 6.7%, respectively). Fukui *et al*. reported that maximum tumor dimension was underestimated (defined as 10 mm or more in pathological tumor dimension compared with radiological ones by preoperative computed axial tomography) in 3.2% of patients without IIPs (5). Park *et al*. compared maximal tumor diameters between fresh pathology specimens and CT images in lung adenocarcinoma and found that postoperative up-staging occurred in 12.3% and 1.4% of tumors on performing radiological staging using axial and multiplanar reformatted CT images (17). In contrast, the honeycombing group in this study had a significantly higher ratio of the tumor size underestimation (33.3%) than did the other groups. Univariate analysis showed that the radiological and pathological maximum tumor sizes were predictive factors for preoperative tumor size underestimation in addition to honeycombing adjacent to the tumor; similar to findings in the study regarding pulmonary emphysema and tumor size underestimation (16). However, multivariate analysis clearly showed that honeycombing adjacent to the tumor was the only statistically significant predictor for the tumor size underestimation.

Sakai *et al*. reviewed the CT scans and pathologic specimens of 57 lung cancer cases in 47 patients with diffuse pulmonary fibrosis for the first time and found that seven tumors invaded the adjacent honeycomb lung histologically and lacked distinct margins on CT images (3). In our study, five cases had tumors that were contiguous with the honeycombed lung and were radiologically underestimated preoperatively; four of these showed tumor infiltration to honeycomb lung or to fibrotic lung tissue adjacent to honeycombed lung on histopathology.

Meanwhile, to discuss causes of the radiological tumor size underestimation in cases of the normal lung group, we divided 628 subjects with normal parenchyma adjacent to the tumor into ones with (n=47) and without (n=581) tumor size underestimation and performed univariate analysis of several risk factors. Pleural invasion of the tumor was significantly more frequent in the patients with tumor size underestimation [12/47 (25.5%)] than in those without underestimation [66/581 (11.4%)] (P=0.01). We examined histopathology of several cases with pleural invasion of the tumor and found that pleural invasion itself did not lead to cause an underestimation of tumor size. The tumors with pleural invasion in the patients with normal parenchyma (n=78) showed significantly larger radiological and pathological maximum tumor sizes than those without pleural invasion (n=550) (radiological, 32.4±15.8 versus 22.9±13.4 mm, P<0.001; pathological, 30.9±15.1 versus 21.1±13.1 mm, P<0.001). At the same time, the patients with tumor size underestimation had significantly larger radiological and pathological tumor sizes than did those without tumor size underestimation (radiological, 29.9±14.2 versus 23.6±13.9 mm, P<0.001; pathological, 47.4±16.4 versus 20.3±11.3 mm, P<0.001). It has been reported that larger tumor size was a risk for radiological tumor size underestimation probably due to difficulties in obtaining the largest cross section of tumors on the CT images (16). Moreover, in other underestimated cases, tumors sometimes extended into narrow lung parenchyma parallel to relatively large sized broncho-pulmonary arterial bundle or into lymphatic vessels along interlobular septum or beneath the pleura, which were not usually visualized on the CT images.

Bland-Altman analysis revealed that the 95% limits of agreement between the pathological and radiological maximum tumor sizes in the patients with honeycombing were 14.7±55.5 mm, i.e., –40.8 to 70.2 mm, indicating that, in 95% of patients with honeycombing adjacent to lung cancer, preoperative radiological underestimation of tumor size can be nearly 70.2 mm. When sub-lobar resection is selected, circumferential margin of at least 35 mm from the tumor should be secured.

Our investigation showed the large difference between lung cancer extent on histopathology and on CT images;

hence, it is not favorable to perform limited surgery for tumors adjacent to honeycombed lungs. Although formalin fixation could affect the tumor size in histopathology (18), this report is the first to show that honeycombing adjacent to the tumor is the major risk of preoperative tumor size underestimation by preoperative examination on CT images. Radiological tumor size underestimation is also important in patients who do not undergo surgery since it could affect the prediction of the patients' prognosis. In the future, we need more accurate diagnostic tools to determine the extension of lung cancer into the adjacent honeycombed lung. A possible candidate for this is the recently advanced dynamic contrast-enhanced MRI with three-dimensional gradient echo (GRE) and ultrashort echo time (UTE) (19,20).

There are some limitations to this study. First, this was a retrospective study conducted at a single institution. Second, the sample size for patients with honeycombing was small. A larger sample size would make the association between the tumor size underestimation and honeycombing more robust. Third, we measured preoperative tumor size on different-sized slices of CT images; mainly on 0.5 mm slices of a CT image, but in some cases, on a 5.0–7.0 mm slices. To discuss a little more about this issue, we divided the subjects into two groups of patients whose tumors were assessed by imaging planes with slice width ≤2 mm (n=786) and ≥5 mm (n=55) and assessed the incidence of preoperative radiological tumor size underestimation in each group. As a result, the incidences of tumor size underestimation in two groups were comparable [≤2 versus ≥5 mm, 64/786 (8.1%) versus 3/55 (5.5%), no statistically significant difference]. However, there is still a possibility of measurement error of the tumor size because of reconstruction thickness. In addition to that, MPR images were available in only some cases. It was reported that tumor size measured on MPR images was more strongly correlated with pathological tumor size than that measured only on axial images (17). Up to thirty-three percent of patients with honeycombing were analyzed only with images in the axial plane, whereas only 13.3%, 15.0%, and 13.4% of patients with reticulation, emphysema, and normal parenchyma were analyzed with the axial images. It might has caused higher incidence of tumor size underestimation in the patients with honeycombing than in those with the other findings. However, as shown in *Table 3*, the proportions of the axial plane (versus MPR) utilized for the analysis of tumor size in the patients with and without tumor size underestimation were comparable (14.4% versus 10.1%, no statistically significant difference). Moreover, multivariate analysis revealed that the imaging plane (only axial plane versus MPR) was not a predictor for tumor size underestimation in this study.

Conclusions

Honeycomb lung adjacent to the tumor is the major risk factor for preoperative radiological tumor size underestimation in patients with lung cancer. It is difficult to accurately measure the extension of tumor into the honeycombed lung areas on CT images. Hence, a suitable resection method should be selected to ensure a curative operation.

Acknowledgments

The authors thank the doctors of the radiology, diagnostic pathology and public health departments of Fujita Health University.
Funding: This work was supported by Fujita Health University research foundation 2021.

Footnote

Reporting Checklist: The authors have completed the STROBE reporting checklist. Available at https://jtd.amegroups.com/article/view/10.21037/jtd-22-1115/rc

Data Sharing Statement: Available at https://jtd.amegroups.com/article/view/10.21037/jtd-22-1115/dss

Peer Review File: Available at https://jtd.amegroups.com/article/view/10.21037/jtd-22-1115/prf

Conflicts of Interest: All authors have completed the ICMJE uniform disclosure form (available at https://jtd.amegroups.com/article/view/10.21037/jtd-22-1115/coif). The authors have no conflicts of interest to declare.

Ethical Statement: The authors are accountable for all aspects of the work in ensuring that questions related to the accuracy or integrity of any part of the work are appropriately investigated and resolved. The study was conducted in accordance with the Declaration of Helsinki (as revised in 2013). This study was approved by the Institutional Review Board of Fujita Health University (CI21-392). The patients viewed an online version of the

consent document and were enrolled in the study using the opt-out method.

References

1. Raghu G, Nyberg F, Morgan G. The epidemiology of interstitial lung disease and its association with lung cancer. Br J Cancer 2004;91 Suppl 2:S3-10.
2. Hubbard R, Venn A, Lewis S, et al. Lung cancer and cryptogenic fibrosing alveolitis. A population-based cohort study. Am J Respir Crit Care Med 2000;161:5-8.
3. Sakai S, Ono M, Nishio T, et al. Lung cancer associated with diffuse pulmonary fibrosis: CT-pathologic correlation. J Thorac Imaging 2003;18:67-71.
4. Lampen-Sachar K, Zhao B, Zheng J, et al. Correlation between tumor measurement on Computed Tomography and resected specimen size in lung adenocarcinomas. Lung Cancer 2012;75:332-5.
5. Fukui M, Takamochi K, Matsunaga T, et al. Risk of the preoperative underestimation of tumour size of lung cancer in patients with idiopathic interstitial pneumonias. Eur J Cardiothorac Surg 2016;50:428-32.
6. Sato T, Teramukai S, Kondo H, et al. Impact and predictors of acute exacerbation of interstitial lung diseases after pulmonary resection for lung cancer. J Thorac Cardiovasc Surg 2014;147:1604-11.e3.
7. Kumar P, Goldstraw P, Yamada K, et al. Pulmonary fibrosis and lung cancer: risk and benefit analysis of pulmonary resection. J Thorac Cardiovasc Surg 2003;125:1321-7.
8. Sato T, Kondo H, Watanabe A, et al. A simple risk scoring system for predicting acute exacerbation of interstitial pneumonia after pulmonary resection in lung cancer patients. Gen Thorac Cardiovasc Surg 2015;63:164-72.
9. Raghu G, Remy-Jardin M, Myers JL, et al. Diagnosis of Idiopathic Pulmonary Fibrosis. An Official ATS/ERS/JRS/ALAT Clinical Practice Guideline. Am J Respir Crit Care Med 2018;198:e44-68.
10. Hansell DM, Bankier AA, MacMahon H, et al. Fleischner Society: glossary of terms for thoracic imaging. Radiology 2008;246:697-722.
11. Bland JM, Altman DG. Statistical methods for assessing agreement between two methods of clinical measurement. Lancet 1986;1:307-10.
12. Kanda Y. Investigation of the freely available easy-to-use software 'EZR' for medical statistics. Bone Marrow Transplant 2013;48:452-8.
13. Tzouvelekis A, Gomatou G, Bouros E, et al. Common Pathogenic Mechanisms Between Idiopathic Pulmonary Fibrosis and Lung Cancer. Chest 2019;156:383-91.
14. Brown SW, Dobelle M, Padilla M, et al. Idiopathic Pulmonary Fibrosis and Lung Cancer. A Systematic Review and Meta-analysis. Ann Am Thorac Soc 2019;16:1041-51.
15. Raghu G, Amatto VC, Behr J, et al. Comorbidities in idiopathic pulmonary fibrosis patients: a systematic literature review. Eur Respir J 2015;46:1113-30.
16. Sugawara H, Watanabe H, Kunimatsu A, et al. Tumor size in patients with severe pulmonary emphysema might be underestimated on preoperative CT. Eur Radiol 2022;32:163-73.
17. Park CH, Kim TH, Lee S, et al. Correlation between maximal tumor diameter of fresh pathology specimens and computed tomography images in lung adenocarcinoma. PLoS One 2019;14:e0211141.
18. Hsu PK, Huang HC, Hsieh CC, et al. Effect of formalin fixation on tumor size determination in stage I non-small cell lung cancer. Ann Thorac Surg 2007;84:1825-9.
19. Hatabu H, Ohno Y, Gefter WB, et al. Expanding Applications of Pulmonary MRI in the Clinical Evaluation of Lung Disorders: Fleischner Society Position Paper. Radiology 2020;297:286-301.
20. Ciliberto M, Kishida Y, Seki S, et al. Update of MR Imaging for Evaluation of Lung Cancer. Radiol Clin North Am 2018;56:437-69.

Cite this article as: Ishizawa H, Matsuda Y, Ohno Y, Sakurai E, Ota A, Hattori H, Tsukamoto T, Matsunaga M, Kawai H, Suzuki Y, Nagano H, Negi T, Tochii D, Tochii S, Suda T, Hoshikawa Y. Honeycomb lung is a major risk factor for preoperative radiological tumor size underestimation in patients with primary lung cancer. J Thorac Dis 2023;15(2):516-528. doi: 10.21037/jtd-22-1115